Long range surface plasmon resonance bacterial pathogen biosensor with magnetic nanoparticle assay

Yi Wang, Wolfgang Knoll and Jakub Dostalek*
Health and Environment
AIT – Austrian Institute of Technology GmbH
Vienna, Austria
*jakub.dostalek@ait.ac.at

Abstract—**In this paper, long range surface plasmons (LRSP) and magnetic iron oxide nanoparticle (MNP) immunoassay are investigated for advancing the sensitivity of surface plasmon resonance (SPR) biosensor technology for the analysis of bacterial pathogens. The MNPs-antibody conjugates served as labels for enhancing the binding-induced refractive index changes and as "vehicles" for rapid delivery of bacteria from a sample solution to the sensor surface by applied magnetic field. A sensor chip for diffraction-coupled long range surface plasmon resonance (LRSPR) was developed and functionalized with capture antibodies. These surface plasmon waves enable improving the resolution of refractive index changes measurements on the surface and probing whole volume of captured bacterial pathogens. The combined LRSPR and MNP assay was applied for detection of *Escherichia coli* O157:H7. About 3 orders of magnitude improvement of the sensitivity with respect to regular SPR and the analysis time of ~30 min are demonstrated. (Abstract)**

I. INTRODUCTION

Surface plasmon resonance (SPR) biosensors were increasingly researched for detection of bacterial pathogens [1]. However, the achieved sensitivity is typically above 10^3 colony forming units (cfu) per mL which is not sufficient for many important applications in areas such as food control and medical diagnostics. The reason is the small binding-induced refractive index changes associated with the capture of the bacterial analyte on the surface. In addition, the analyte mass transfer to the sensor surface is strongly hindered by a slow diffusion owing to the micrometer size of bacterial pathogens and the bacteria captured on the surface are exposed to a shear stress which results in the destabilization of the bonding between catcher and analyte molecules. A surface architecture that supports long range surface plasmons (LRSPs) has been shown to improve the sensitivity for the detection of bacteria owing to the larger penetration depth and higher figure of merit in the refractive index changes measurements [2]. Magnetic nanoparticles (MNPs) were combined with SPR for the detection of molecular analytes [3-6] and they are extremely attractive for the analysis of bacterial pathogens as they can serve for concentration/purification of bacteria from complex samples as well as for an enhancement of the refractive index changes [7]. Furthermore, MNPs offer the opportunities to quickly deliver target analyte to the sensor surface under magnetic field gradient, thus overcome the diffusion limited mass transfer [8]. In this paper, we demonstrate the combined LRSPR and MNP assay for the detection of *Escherichia coli* O157:H7.

II. MATERIALS AND METHODS

A. Materials

Magnetic iron oxide nanoparticles modified with polysaccharide layer (fluidMAG-ARA with diameter of ~200 nm, magnetic core diameter of ~175 nm) were purchased from Chemicell (Berlin, Germany). *E. coli* O157:H7 standard was obtained from KPL (Gaithersburg, MD). The average diameters of heat-killed *E. coli* O157:H7 were determined by dynamic light scattering (DLS) with Zetasizer from Malvern Instruments (Worcestershire, UK) as 1177 nm. Capture antibodies against *E. coli* O157:H7 (c-ab) (cat. No. ab75244) were purchased from Abcam (Cambridge, UK). Affinity-purified detection antibodies (d-Ab) against *E. coli* O157:H7 (cat. No. 01-95-90) were obtained from KPL. 1-ethyl-3-(3-dimethylaminopropyl)carbodiimide (EDC) and N-hydroxysuccinimide (NHS) were from Pierce (Rockford, USA). Dithiolaromatic PEG6-carboxylate (thiol-COOH) and dithiolaromatic PEG3 (thiol-PEG) were purchased from SensoPath Technologies (Bozeman, USA). 2-(N-Morpholino)ethanesulfonic acid (MES), PBS buffer tablets and Tween-20 were purchased from Sigma-Aldrich. PBS-Tween buffer (PBST) was prepared by adding Tween 20 (0.05%) in PBS buffer solution. Cylindrical magnets (NdFeB) with diameter of 10 mm and length of 25 mm were purchased from Neotexx (Berlin, Germany).

B. Optical setup

There was used an SPR biosensor setup that is depicted in Fig. 1A. A light beam He-Ne laser passed through a chopper and a polarizer to select transversal magnetic (TM) polarization and was reflected at a surface of a diffraction grating sensor chip. The assembly of the sensor chip and flow-cell was mounted on a rotation stage (Huber AG, Germany) in order to control the angle of incidence θ. The intensity of the laser beam reflected at the sensor surface was measured by using a photodiode (PD) connected to a lock-in amplifier (Princeton Applied Research, USA). A cell with the volume 10 μL, length L=10 mm and depth h=0.1 mm was attached against the sensor chip to flow liquid samples at the flow rate of 503 μL min^{-1}. For the MNP immunoassays, an external magnetic field with a gradient perpendicular to the surface of ∇B=0.10 T mm^{-1} was applied by using a 1.4T NdFeB cylindrical magnet (diameter of 10 mm, length of 25 mm from Neotexx, Berlin, Germany) placed at the distance of 2 mm from the sensor surface.

978-1-4244-9837-6/11/$26.00 ©2011 IEEE

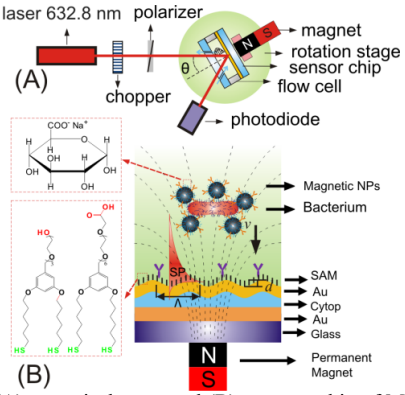

Fig.1 Scheme of (A) an optical setup and (B) a sensor chip of MNP-enhanced diffraction-coupled LRSPR for the detection of bacteria.

C. *Sensor chips*

Diffraction grating sensor chips for SPR and LRSPR were prepared by nano-imprint lithography from a silicon master (sinusoidal relief modulation grating with period of Λ=520 nm and depth of d=58-64 nm) that was casted to a PDMS stamp. On the sensor chip supporting diffraction-coupled regular SPR, the motif on a soft stamp was transferred to UV-curable polymer (NOA72, Netherland) and coated with a thin gold layer (thickness of 60 nm) by using sputtering (UNIVEX 450C from Leybold Systems, Germany). For the diffraction-coupled LRSPR, a 100 nm Au was sputtered on a glass slide followed by spin-coating of a low-refractive index polymer (Cytop from Asahi, Japan) with the thickness of 630 nm. After 5-min drying, PDMS stamp was used to transfer the grating structure to the Cytop layer upon the curing at 50 °C overnight. Afterwards, the PDMS stamp was peeled off and the Cytop layer was coated with 25 nm thick gold layer. Thiol SAM was formed on the gold covered SPR and LRSPR chips by overnight incubating in a mixture of thiol-COOH and thiol-PEG dissolved at molar ratio of 1:9 in absolute ethanol (total concentration of 1 mM). Afterwards, the gold surface was rinsed with ethanol and dried in a stream of N_2. The capture antibody (c-Ab) was immobilized on the sensor surface by EDC/NHS.

D. *Modification of magnetic nanoparticles with antibodies*

MNPs were modified with dAb according to the protocol from supplier The antibody-to-MNP ratio was estimated as 10:1, assuming 90% of antibodies were immobilized on the MNPs surface during the labeling process [9].

E. *Detection formats*

The changes of the reflectivity R were recorded in time at a fixed angle with the highest slope of the SPR reflectivity dip (see Fig.2A). In direct detection format, PBS samples spiked with *E. coli* O157:H7 were flowed over the sensor surface with immobilized c-Ab. After 15-min circulation, the sensor surface was rinsed with PBS. Sensor response was determined as the reflectivity change before and after the flow of target analyte. For the MNPs immunoassay MNP-abs conjugates (0.01 mg ml^{-1} after incubation) were incubated with *E. coli* O157:H7 in PBS for about 15 min. Afterwards, the mixture was circulated through the flow cell for 10 min with applied magnetic field gradient ∇B=0.10 T mm^{-1}. After 1-min rinsing with PBS, the magnet was removed from the sensor surface, and the reflectivity change was determined after 3 min. After the analyte binding, 10 mM NaOH was employed for the regeneration of the sensor surface. The LOD was determined as the concentration at which the response ΔR is equal to 3 times of the standard deviation of reflectivity signal 3σ(R), $\sigma(R)= 2.5\times10^{-4}$.

III. Results and Discussions

A. *Refractometric study of SPR and LRSPR*

Firstly, a refractometric study was performed in order to compare the accuracy of the measurements of refractive index changes by diffraction-coupled SPR and LRSPR. In this experiment, samples with increasing refractive index (PBS spiked with ethylene glycol - EG) were successively flowed through the sensor. As shown in Fig. 2A, the increasing refractive index δn is associated with a shift of the resonance dip towards higher angles of incidence $\delta\theta$. The angular sensitivity to bulk refractive index ($S=\delta\theta/\delta n$) was determined for diffraction-coupled LRSPR and SPR as S=38 deg RIU^{-1} and S=92 deg RIU^{-1}, respectively. As the full width in half minimum (FWHM) of the LRSPR ($\Delta\theta$=0.3 deg) is 12-fold lower compared to that of regular SPR ($\Delta\theta$=3.6 deg), the figure of merit (FOM, defined as $\chi=S/\Delta\theta$) was about 5 times larger for LRSPR (χ=127) compared to regular SPR (χ=26). The real-time monitoring of the reflectivity changes (at an incident angle with highest slope θ=9.85 deg for SPR and θ=3.27 deg for LRSPR) enabled measuring the refractive index changes with a slope of $S_R=\Delta R/\delta n$ of 119 and 14 RIU^{-1} for LRSPR and SPR, respectively (Fig. 2B). Based on the $\sigma(R)= 2.5\times10^{-4}$, the resolution was 8.5 fold higher for LRSPR (2.1×10^{-6} RIU) than for regular SPR (1.8×10^{-5} RIU).

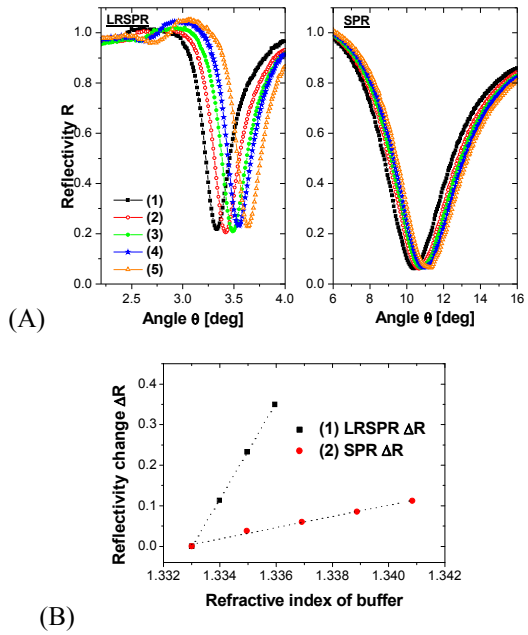

Fig.2 (A) Angular reflectivity spectra for a diffraction-coupled LRSPR sensor chip and a diffraction-coupled regular SPR sensor chip in contact with PBS buffer spiked with ethylene glycol at the concentration from (1) 0, (2) 2%, (3)

4%, (4) 6%, and (5)8%. (B) Comparison of diffraction-coupled SPR and LRSPR on the reflectivity changes to the changes of bulk refractive index.

B. Detection of E. coli O157:H7

Fig. 3 shows the angular spectra before and after the capture of *E. coli* O157:H7 at concentration of 10^6 cfu/mL for diffraction-coupled LRSPR and regular SPR. It shows that the analyte binding is accompanied with a resonance shift of 0.2 deg and 0.12 deg for SPR and LRSPR, respectively. However owing to the 12-fold lower FWHM, the reflectivity change for LRSPR is about 3-fold higher (at 3.14 deg) than that for regular SPR measurement (at 12.5 deg). Let us note that the small decrease in the overall reflectivity is caused by the scattering of the MNP-bacteria aggregates which were bound on the sensor surface.

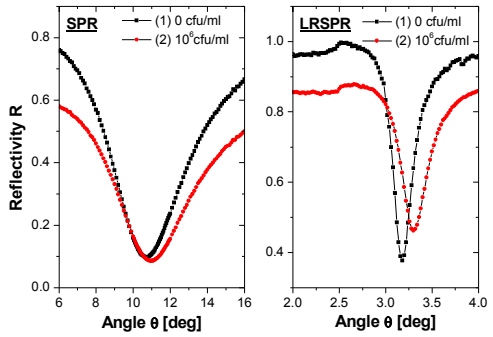

Fig.3 Angular reflectivity spectra of a diffraction-coupled LRSPR regular SPR sensor chip before and after the capture of *E. coli* O157:H7 (MNPs immunoassay with analyte concentration 10^6 cfu/ml)

Direct and MNPs-enhanced detection of *E. coli* O157:H7 was investigated for the diffraction-coupled regular SPR. The time-dependent reflectivity changes were recorded at the incident angle of 12.5 deg. The reflectivity changes ΔR were measured in triplicate for samples with target analyte dissolved at concentrations between 10^3 and 10^6 cfu/mL. The obtained calibration curves for direct and MNP-enhanced detection format are shown in Fig. 4. From these data, the limit of detection (LOD) was determined as 6.5×10^5 cfu/ml and 10^3 cfu/ml for direct detection and MNPs immunoassay of *E. coli* O157:H7, respectively.

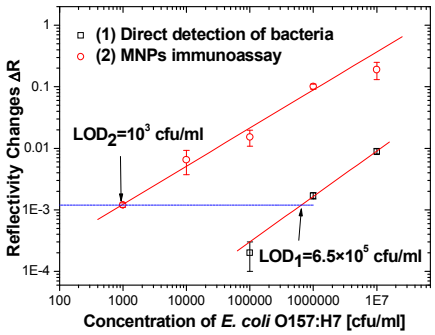

Fig. 4 The calibration curve for (1) direct detection and (2) MNPs immunoassay of *E. coli* O157:H7 based on diffraction-coupled regular SPR.

IV. CONCLUSIONS

A new SPR sensor platform based on diffraction-coupled long range surface plasmon resonance (LRSPR) was developed for MNP immunoassays in which magnetic field gradient can be applied through the chip. The refractometric study was carried out showing about 5-times improved figure of merit of LRSPR with respect to regular SPR. This feature resulted in 8.5-fold lower refractive index resolution for LRSPR compared to regular SPR architecture. The sensor platform was employed for the detection of *E. coli* O157:H7 based on immunoassays. With respect to direct detection format, magnetic nanoparticle-enhanced format allowed improving the sensitivity for *E. coli* O157:H7 detection by almost three orders of magnitude from 6.5×10^5 cfu/ml to 10^3 cfu/ml for diffraction-coupled regular SPR. The assay based on LRSPR was shown to increase the signal strength associated with the bacteria binding with a factor of three. The future work will be devoted to combining of LRSPR with magnetic nanoparticle assays for ultrasensitive detection of bacterial pathogens in realistic samples.

ACKNOWLEDGMENT

The authors would like to acknowledge the partially support for this work provided by ZIT, Center of Innovation and Technology of Vienna.

REFERENCES

[1] J. Homola, "Surface plasmon resonance sensors for detection of chemical and biological species," *Chem.Rev.,* vol. 108, pp. 462-493, Feb 2008.

[2] M. Vala, *et al.*, "Long-range surface plasmons for sensitive detection of bacterial analytes," *Sensors and Actuators B-Chemical,* vol. 139, pp. 59-63, May 2009.

[3] J. S. Mitchell, *et al.*, "Sensitivity enhancement of surface plasmon resonance biosensing of small molecules," *Anal. Biochem.,* vol. 343, pp. 125-135, Aug 2005.

[4] J. L. Wang, *et al.*, "Magnetic Nanoparticle Enhanced Surface Plasmon Resonance Sensing and Its Application for the Ultrasensitive Detection of Magnetic Nanoparticle-Enriched Small Molecules," *Anal. Chem.,* vol. 82, pp. 6782-6789, Aug 2010.

[5] P. Tseng, *et al.*, "Rapid and Dynamic Intracellular Patterning of Cell-Internalized Magnetic Fluorescent Nanoparticles," *Nano Letters,* vol. 9, pp. 3053-3059, Aug 2009.

[6] Y. Teramura, *et al.*, "Surface plasmon resonance-based highly sensitive immunosensing for brain natriuretic peptide using nanobeads for signal amplification," *Anal. Biochem.,* vol. 357, pp. 208-215, Oct 15 2006.

[7] S. D. Soelberg, *et al.*, "Surface Plasmon Resonance Detection Using Antibody-Linked Magnetic Nanoparticles for Analyte Capture, Purification, Concentration, and Signal Amplification," *Anal. Chem.,* vol. 81, pp. 2357-2363, Mar 2009.

[8] Y. Wang, *et al.*, "Magnetic Nanoparticle-Enhanced Biosensor Based On Grating-Coupled Surface Plasmon Resonance," *Anal. Chem.,* submitted.

[9] I. Koh, *et al.*, "Magnetic iron oxide nanoparticles for biorecognition: Evaluation of surface coverage and activity," *J. Phy. Chem. B,* vol. 110, pp. 1553-1558, Feb 2 2006.